



Cite this: *Environ. Sci.: Processes Impacts*, 2025, **27**, 3107

## Ferrihydrite level in paddy soil affects inorganic arsenic species in rice grains

Arindam Malakar, <sup>a</sup> Daniel D. Snow, <sup>a</sup> Michael Kaiser, <sup>c</sup> Harkamal Walia, <sup>c</sup> Trenton L. Roberts<sup>d</sup> and Chittaranjan Ray<sup>\*b</sup>

Rice is consumed by ~50% of the global population, grown primarily in flooded paddy fields, and is susceptible to arsenic accumulation. Inorganic arsenic, particularly in reduced form (As(III)), is considered the most toxic and is more likely to accumulate in rice grains under flooded systems. We postulate that increased levels of highly reactive iron minerals, such as ferrihydrite, in paddy soils can regulate the bioavailability of arsenic and reduce its uptake by priming iron plaque formation. To clarify, two rice varieties, Norin and Sabharaj, differing in arsenic uptake rate, were grown in paddy soil under flooded conditions with arsenate (As(V)) spiked-irrigation water. 2-line ferrihydrite was added at 0.00% (control), 0.05%, and 0.10% w/w and served as the highly reactive iron species. Irrespective of rice varieties, total inorganic arsenic (As(III) + As(V)) in grains in ferrihydrite systems decreased by 85 to 93% compared to the control. These results support ferrihydrite's intrinsic role in controlling paddy soils' rhizosphere chemistry. Our findings indicate that fresh reactive iron minerals are critical in the early formation of root iron plaque, which enhances the defense mechanism against arsenic. The findings may have implications for reducing toxic inorganic arsenic accumulation in lowland rice.

Received 18th June 2025  
Accepted 1st September 2025

DOI: 10.1039/d5em00475f

rsc.li/espi

### Environmental significance

Naturally occurring arsenic in soil and irrigation water used for rice production accumulates in harvested rice grains. Though flooded irrigation is primarily used in rice production, it is unclear how reactive iron minerals, such as ferrihydrite, concentration in soil affects arsenic uptake, specifically the most toxic inorganic arsenic species within the root-soil-water continuum. As rice is the staple food of half of the world's population, understanding rice rhizosphere geochemistry to minimize inorganic arsenic uptake cannot be overstated. Here, we identify that a slight increase in reactive iron concentrations significantly decreases inorganic arsenic, and specifically the more toxic arsenite species, accumulation in rice grains, which can be a viable solution to reduce inorganic arsenic accumulation in rice.

## 1. Introduction

Rice is a critical food source for more than 50% of the global population, making safe future production essential.<sup>1</sup> Rice produced in flooded production systems faces contamination from arsenic (As) occurrence in soil and/or irrigation water, which leads to potentially harmful accumulation in rice grain.<sup>2</sup> Arsenic, a known carcinogen,<sup>3</sup> is considered an imminent health threat to humans consuming rice as their staple food.<sup>4</sup> Arsenic exists in several forms<sup>5</sup> and its inorganic states,

particularly arsenite (As(III)), are the most toxic, surpassing the toxicity of organic forms (though methylated arsenic is considered carcinogenic).<sup>6</sup> Since inorganic arsenic accumulates in rice grains,<sup>6</sup> consuming rice with elevated levels of arsenic poses serious health risks. This is a global phenomenon,<sup>7</sup> and we urgently need new agricultural practices to control inorganic arsenic levels in rice grains.

Research directed to exploring methods to reduce arsenic levels in rice include genetic engineering (varying rice cultivars)<sup>8</sup> and growing rice in well-aerated soil, such as alternate wetting and drying.<sup>9</sup> One intrinsic way rice plants control arsenic uptake is by forming iron plaque on the root surface.<sup>10</sup> Rice roots develop iron plaque when oxygen is released into the rhizosphere from the roots.<sup>11</sup> Iron plaque in flooded conditions primarily retains arsenate (As(V)) (80–82%), with smaller amounts of arsenite (As(III)) (18–20%)–iron (oxyhydr)oxide complexes.<sup>11</sup> This plaque comprises amorphous or crystalline iron (oxyhydr)oxides, primarily ferrihydrite (Fh),<sup>12,13</sup> while lepidocrocite and goethite are also observed.<sup>14</sup> Mitigation strategies such as alternate wetting and drying of rice fields increase soil

<sup>a</sup>Nebraska Water Center, Daugherty Water for Food Global Institute and School of Natural Resources, University of Nebraska, Lincoln, Nebraska 68583-0844, USA. E-mail: amalakar2@unl.edu

<sup>b</sup>Nebraska Water Center, Part of the Robert B. Daugherty Water for Food Global Institute 2021 Transformation Drive, University of Nebraska, Lincoln, Nebraska 68588-6204, USA. E-mail: cray@nebraska.edu

<sup>c</sup>Department of Agronomy and Horticulture, University of Nebraska-Lincoln, Lincoln, Nebraska 68583-0915, USA

<sup>d</sup>Department of Crop, Soil and Environmental Sciences, University of Arkansas, Fayetteville, Arkansas 72701, USA



aeration and the influx of oxygen, which may promote the formation of iron plaque around the roots, and can also favor arsenic oxidation and reduce bioavailability, thereby preventing arsenic from being transformed into a more soluble, reduced, and toxic arsenite.<sup>15</sup> Unlike alternating wetting and drying, creating well-aerated soil under continuous flooding conditions is not feasible. Another strategy is supplementing the soil with iron oxides/hydroxides in flooded rice fields, which can trap arsenate on their surfaces and make it less available to plants.<sup>16,17</sup> However, iron mineral dissolution is possible under reducing conditions prevalent in flooded rice soils.<sup>17-19</sup>

Flooded rice cultivation, the major form of rice production,<sup>20</sup> induces the reductive dissolution of soil iron minerals, releasing sequestered arsenic and potentially leading to arsenic accumulation in grains.<sup>21,22</sup> While arsenite and arsenate exist in paddy soil and soil solutions, arsenite dominates under flooded conditions. However, the physiochemical conditions of the rhizosphere, which are dependent on the rice cultivar,<sup>23</sup> differ significantly from the bulk soil due to root oxygen release and iron plaque formation. An oxidative rhizosphere potentially changes arsenic speciation near the root surface.<sup>23</sup> Few studies have examined how arsenic species concentration varies in rice grains due to the variation in the concentration of iron plaque formed on rice roots.<sup>14,18,24-27</sup> However, there is a lack of information on how different soil concentrations of reactive iron minerals,<sup>28,29</sup> such as ferrihydrite (Fh), promote plaque formation, ultimately affecting arsenic species in the rice grain.

Elucidating the role of iron plaque and the occurrence of reactive iron species can lead to a mitigation strategy to reduce inorganic arsenic in rice grains. We hypothesize that adding reactive iron minerals such as Fh, which is one of the primary components of iron plaque, to paddy soil will promote an early onset of iron plaque formation around rice roots, impacting arsenic uptake and speciation in the mature rice grain. A faster formation of a protective layer of iron plaque will likely immobilize arsenic and potentially reduce arsenic bioavailability, plant uptake, and accumulation. Further, the iron plaque layer can preferentially adsorb and sequester arsenate, making it less available for reduction to arsenite. Since rice uptake varies by rice cultivar,<sup>8</sup> understanding rhizosphere chemistry-based arsenic speciation under different rice cultivars is crucial for determining how reactive iron minerals impact adsorption. This study evaluates the effects of small additions and fluctuations of reactive iron levels in paddy soil on arsenic species and uptake in mature rice grains.

## 2. Materials and methods

### 2.1 Materials

Reagents, including iron(III) chloride ( $\text{FeCl}_3$ ) reagent grade (97%), sodium bicarbonate (ACS reagent, >99.7%,  $\text{NaHCO}_3$ ), trisodium citrate dihydrate (ACS reagent, ≥99%), ferrous sulfate (99.9%), ammonium acetate (99.9%), acetic acid (99.9%), calcium carbonate (ACS reagent, ≥99%), sodium nitrite (ReagentPlus®, ≥99.0%), and 1,10-phenanthroline (99.9%) were purchased from Sigma-Aldrich, USA. Sulfanilamide (Certified ACS, Fisher Chemical), *N*-(1-naphthyl)

ethylenediamine, dihydrochloride (98+, ACS reagent), zinc acetate dihydrate ( $\text{Zn}(\text{CH}_3\text{COO})_2 \cdot 2\text{H}_2\text{O}$ ) (extra pure, 98%), ammonium carbonate (ACS reagent,  $(\text{NH}_4)_2\text{CO}_3$ ), sodium hydrosulfite (ca. 85%, Tech.,  $\text{Na}_2\text{S}_2\text{O}_4$ ), and potassium hydroxide (KOH) were manufactured by ACROS organics™ and purchased from Fisher Scientific, USA. Arsenic and uranium standards were purchased from Inorganic™ Venture, USA. Arsenite (As(III)) and Arsenate (As(V)) reference standards were purchased from Millipore Sigma, USA. All water used in the experiment was reagent grade with a resistivity of 18.2  $\text{M}\Omega \text{ cm}^{-1}$ .

### 2.2 Synthesis of 2-line ferrihydrite

2-line ferrihydrite (Fh) synthesis followed the method described elsewhere.<sup>30</sup> Briefly, 25 g of  $\text{FeCl}_3$  salt was dissolved in 10 L of reagent-grade water. The pH of this solution mixture was brought to near neutral by the controlled addition of KOH, and the pH was kept around  $\sim 6.5 \pm 0.2$ . Finally, 0.15 g of  $\text{Zn}(\text{CH}_3\text{COO})_2 \cdot 2\text{H}_2\text{O}$  was added to change the zeta potential of the solution. The whole mixture was shaken well to precipitate 2-line Fh. The solution was decanted and filtered to reduce volume. The precipitate was dried in a vacuum desiccator kept at room temperature for 48 hours before use. Multiple synthesis batches were carried out to produce all the 2-line Fh required for the greenhouse experiment. Powder XRD (PANalytical Empyrean Diffractometer, Cu  $\text{K}\alpha$  source) was carried out to confirm the formation of 2-line Fh, which matches well to the (110) and (115) planes of 2-line Fh (Fig. S1, PCPDF# 29-0712).<sup>30,31</sup>

### 2.3 Greenhouse experiment

Rice was grown under a continuously flooded irrigation system under controlled temperature, light, and humidity. The soil used to grow rice was collected from a rice field located in Stuttgart, Arkansas ( $34^{\circ}4.6' \text{ N}$ ,  $91^{\circ}40.6' \text{ W}$ ) at the Rice Research Center at the University of Arkansas. The collected soil is classified as Dewitt silt loam (fine, smectitic, thermic Typic Albaqualf).<sup>32</sup> The soil pH was  $7.2 \pm 0.2$ , containing 0.7% total C,  $4.7 \pm 0.7 \text{ mg kg}^{-1}$  arsenic and  $80.8 \pm 7.0 \text{ g kg}^{-1}$  iron. The soil was air-dried in a greenhouse and sieved through a 2 mm mesh before the start of the experiment.

Seven kilograms of air-dried sieved soil (contributing  $\sim 32.9 \text{ mg}$  arsenic from the soil/pot) were weighed out in a polyethylene planting bag ( $n = 300$ ) of 15 cm in diameter and 32 cm in length; multiple holes were made in the bag for easy entry of irrigation water, which was placed in polyethylene tree pots of the same dimension (Fig. 1a, day 0). Rice was grown under continuously flooded irrigation conditions. Pots were submerged in a tub (internal dimension:  $36.4 \times 35.6 \times 58.4$ ,  $\sim 102 \text{ L}$  (27 gals) polypropylene tote box (HDX, Marietta, GA)) filled with 35 cm of arsenic-spiked irrigation water in a greenhouse (10 pots in each tub) to create flooded irrigation conditions.<sup>33</sup> Irrigation water was filtered tap water and spiked with arsenate solution to produce  $50 \text{ }\mu\text{g L}^{-1}$  final arsenic concentration. A total mass of  $\sim 3.6 \text{ mg}$  of arsenic as arsenate was contributed from irrigation water in each tub (0.36 mg from irrigation water/pot), compared to  $\sim 32.9 \text{ mg}$  of arsenic from the



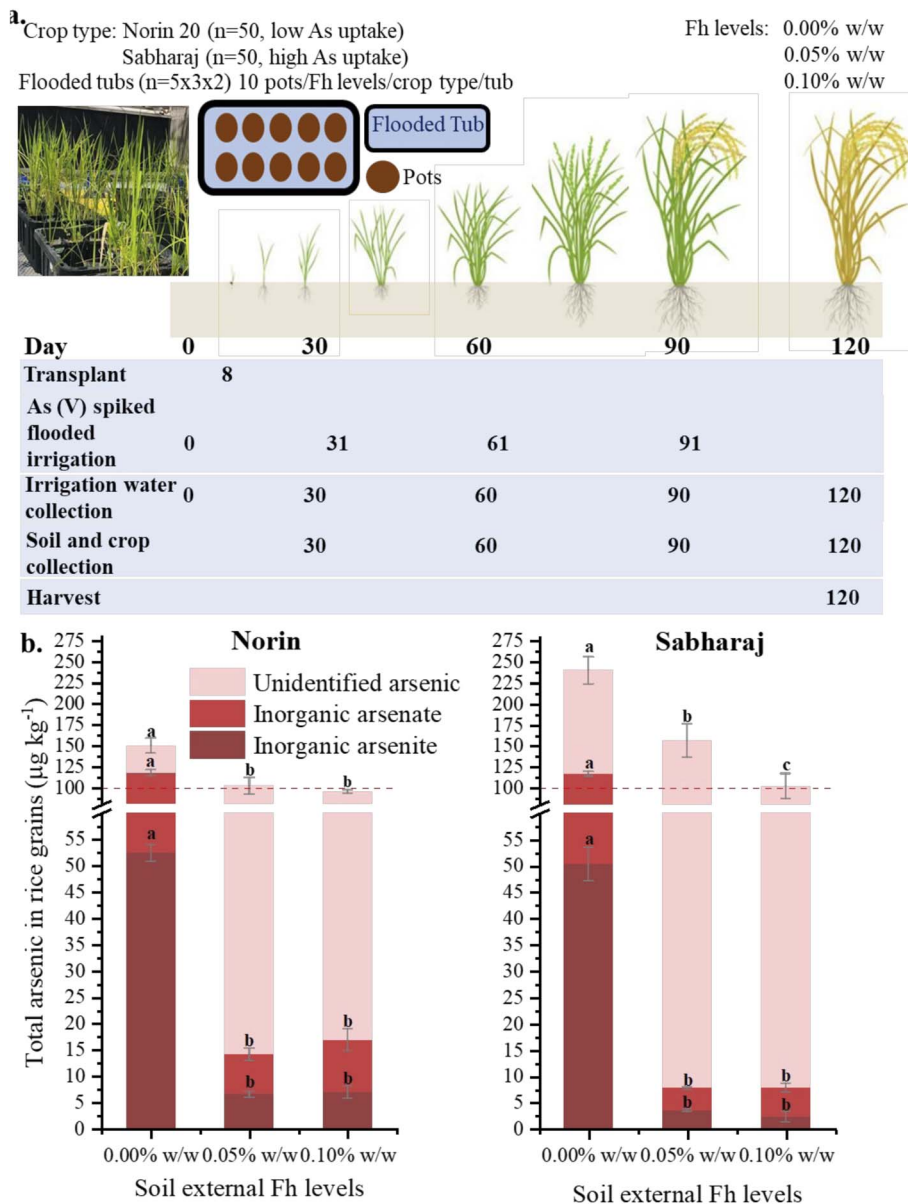


**Fig. 1** (a) Timeline of water sampling from 30 tubs, soil and crop sampling, and final harvesting in the greenhouse experiment. The blue rectangle shows the flooded tub where the ten pots (brown circles) were submerged to create a continuously flooded system (on left: an actual picture of the tub setup) (b) total arsenic uptake in rice grains of two rice varieties, Norin and Sabharaj, where arsenic uptake is divided into arsenite, arsenate, and unidentified arsenic species. Each arsenic species is individually compared for significant differences, and the letters a, b, and c denote  $p < 0.01$  differences as per post hoc Tukey's test. Elevated ferrihydrite (Fh) levels in the soil promote unidentified arsenic species uptake while significantly ( $p < 0.01$ ) reducing inorganic arsenic species in rice grains.

soil per pot ( $\sim 329$  mg from 10 pots in a tub) in each system. The arsenic content of irrigation water was chosen at  $50 \mu\text{g L}^{-1}$ , as it is the drinking water standard for many developing countries,<sup>34</sup> and also to keep arsenic from irrigation water as a significantly small component compared to arsenic in paddy soil used in the experiment. Arsenic-spiked water pH was  $7.6 \pm 0.1$ , total alkalinity was  $174 \pm 12 \text{ mg kg}^{-1}$ , and total dissolved solids (TDS) were  $365 \pm 23 \text{ mg kg}^{-1}$ . Dissolved iron was below detection, and the concentration of arsenate was  $49.5 \pm 1.1 \mu\text{g L}^{-1}$ , arsenite was  $0.8 \pm 0.1 \mu\text{g L}^{-1}$  and total arsenic was  $50.2 \pm 2.1 \mu\text{g L}^{-1}$ . Irrigation water composition is available in SI Table S1. After

every sampling event, the irrigation water was completely discarded and refilled to a 35 cm level in each tub to ensure the same water volume and arsenate concentration in each tub after sampling events.

A set of 10 tubs was used as the control and these pots received no Fh (control = 0.00% w/w,  $n = 100$  pots). Another set of 10 tubs contained pots receiving 0.05% w/w Fh ( $n = 100$  pots), and the final set of 10 tubs had pots that received 0.10% w/w Fh ( $n = 100$  pots) to spike reactive iron concentration of the paddy soil. The synthesized Fh was weighed out and dispersed in 50 g of reagent-grade water. The Fh-water mix was directly applied

on the top of the soil in the pots and mixed with the topsoil (~5 cm). In the control pots, only 50 g of reagent-grade water was applied. The pots with added Fh and flooded tubs were left to equilibrate for a week before transplanting rice seedlings.

Each set of ten tubs was further divided into two groups for two rice (*Oryza sativa* L.) varieties: Sabharaj (*indica*) ( $n = 5$  tubs (10 rice plant per tub), a total of 15 tubs for three Fh levels), known to accumulate high concentrations of arsenic, and Norin 20 (*Temperate japonica*, which will be termed as Norin from now on) ( $n = 5$  tubs (10 rice plant per tub), a total of 15 tubs for three Fh levels), known to accumulate low concentrations of arsenic.<sup>32</sup> Dehusked rice seeds were surface sterilized by soaking them for 30 minutes in 30% bleach and rinsing them with sterilized water. After this, seeds were placed on half-strength Murashige and Skoog media and incubated at 28 °C for two days in the dark, followed by six days in the light.<sup>35</sup> After this, similar-sized seedlings ( $n = 3$ ) were transplanted to paddy field soil pots on day 8 (Fig. 1a).<sup>36</sup> Following transplantation, the germination of rice seedlings was monitored for three days and thinned to one plant per pot after proper growth. Rice was grown for 120 days, and mature grains were formed by the end of the experiment. The greenhouse temperature was maintained between 23 and 34 °C. The crops received 16 hours of light, the maximum level for the summer growing season. The remaining greenhouse space was filled with water tubs to maintain relative humidity (RH) above 50%, recorded every 30 minutes. The floor was sprayed with water every morning and evening to maintain the RH, which averaged  $52 \pm 17\%$  throughout the experiment.

#### 2.4 Irrigation pore water, soil, and plant tissue sampling and analyses

Water samples from the tubs, soil, and plant sampling events were collected on days 30, 60, 90, and 120 (Fig. 1a). Due to the continuously flooded condition and sufficient time between sampling events, it was assumed that water in the tubs established a dynamic equilibrium with the pore water in the soil.<sup>37-40</sup> Pore water samples from each tub at ~20 cm depth from the soil surface were collected from the pots directly and filtered using a 0.45 µm syringe filter. Since colloidal iron could be present,<sup>41</sup> we analyzed the samples immediately for reduced iron ( $\text{Fe}^{2+}$ ) colorimetrically.<sup>42</sup> Total alkalinity, dissolved organic carbon (DOC), major anions, and inorganic arsenic species were measured within 48 hours of sample collection.<sup>43,44</sup> Pore water was subsampled and preserved with sulfuric acid to measure nitrate and ammonium, and preserved with hydrochloric acid to measure total arsenic, total iron, and major cations.

Soil pH, by 1 : 1 soil : water solution (Oakton PHTestr 30) and oxidation-reduction potential (ORP) (Extech RE300 ExStik ORP meter) were measured twice a week in each pot. Soil samples were collected after pore water sampling from each tub ( $n = 5$  per treatment per cultivar), and on day 120, all remaining pots ( $n = 35$ ) were sampled. These were analyzed for dithionite-citrate-bicarbonate (DCB) extractable iron, acid-leachable iron, and total dissolved arsenic using inductively coupled plasma mass spectrometry (ICP-MS) using a Thermo iCAP RQ ICP MS

(Thermofisher Scientific, Waltham, MA USA).<sup>31</sup> Soil Certified Reference Materials (CRMs) were periodically extracted and analyzed, and the results were within  $\pm 5\%$  of the certified values. A more detailed description of all analyses is available in the SI.

Plants ( $n = 5$  per treatment per cultivar (days 30, 60, and 90) and  $n = 35$  on day 120) were harvested with the soil samples. After washing and drying, the biomass and separated roots, shoots, and grains (where applicable) were recorded. Dried plant tissues (at 65 °C) were ground, and DCB-extractable iron and total iron were measured using ICP-MS, which was also used to determine the concentrations of trace elements within the plant tissues.<sup>45</sup> Total arsenic in dried rice grains was measured in ICP-MS<sup>46</sup> after microwave digestion. Approximately 0.5 g of ground and sieved sample was taken in a Teflon™ tube, and 5 mL of high-purity nitric acid (TraceMetal™ Grade, Fisher Chemical, Waltham, MA, USA), hydrochloric acid (Trace-Metal™ Grade, Fisher Chemical, Waltham, MA, USA), and hydrogen peroxide (Sigma-Aldrich, St. Louis, MO, USA) were added. It was digested in a MARS Xpress microwave digestor (CEM, Matthews, NC, USA). After digestion, samples were filtered (0.45 µm, PES w/PP, Whatman GD/XPTM Syringe Filters, GE Healthcare, Chicago, IL, USA); added 0.500 mL of 100 µg·In L<sup>-1</sup>, and diluted to a final volume of 50.0 mL ultrapure deionized water (18.2 MΩ, Barnstead/Thermolyne Nanopure Diamond Water Purification System, Dubuque, IA, USA) before analysis.

Arsenic species, which may include inorganic arsenic fractions (As(III) and (V)), as well as monomethyl arsenate (MMA) and dimethyl arsenate (DMA) in dried rice tissues, including grains, were extracted using a method known to preserve inorganic and organic arsenic species<sup>47</sup> and were separated with a Dionex ICS-5000+ ion chromatography system (IC) (with IonPac AG7 (guard column 2 × 50 mm) + IonPac AS7 (2 × 250 mm)) and measured using IC-ICP-MS.<sup>47-49</sup> Briefly, 1.5 g of dried and sieved rice grains was taken in a 50 mL polypropylene tube, and 15 mL of 0.28 M nitric acid was added, which was extracted at 95 °C for 90 minutes.<sup>47</sup> The extracted arsenic species were separated in the IC, where two mobile phase gradient eluent was created using 20 mmol L<sup>-1</sup> and 200 mmol L<sup>-1</sup> ammonium carbonate (starting at 100% 20 mmol L<sup>-1</sup>, changing to 100% 200 mmol L<sup>-1</sup>, in a linear gradient over 15 min. at 30 °C).<sup>50</sup> The results were confirmed using reference material (NIST Standard Reference Material (SRM) 1568b US (Arkansas) long grain rice flour), and recovery ranged from 92% to 108% (Table S2). Bioaccumulation and transfer factors (formula available in SI) were also calculated for rice varieties and all treatments to understand the movement and accumulation of arsenic within the plants.

#### 2.5 Statistical analyses

Data generated in the study were plotted in Origin Pro (Version 2023b, OriginLab Corporation, USA), which was also used for all statistical analyses. Data included in the article and SI are presented as mean  $\pm$  standard deviation, and error bars in figures represent standard deviation. Before analysis, data were



checked for normal distribution and homogeneity of variance. Pearson correlation coefficients and one-way ANOVA with Tukey post-hoc tests were used to determine the statistical significance of the addition of soil with Fh levels (0.00%, 0.05%, and 0.10% Fh) on selected parameters.

## 2.6 Chemical equilibrium modeling

The USGS chemical thermodynamics program PHREEQC (version 3) evaluated mineral and species equilibrium.<sup>51</sup> A wateq4f.dat database relevant to arsenic and iron species<sup>52</sup> was utilized to predict expected species present during sampling. Measured parameters and ion concentrations were used to develop the chemical equilibrium model. Model inputs included measured temperature, pH, alkalinity, major anions and cations, ammonia, and the total concentrations of iron and arsenic. Reduced iron and arsenite data were not used as input, but measured concentrations of reduced iron and arsenite were used to validate the model.<sup>31,53</sup>

## 3. Results and discussion

### 3.1 Soil ferrihydrite concentrations affect arsenic species in water, soil, and plant tissues

Rice grain harvested at the end of the study was digested and analyzed for arsenite, arsenate, inorganic arsenic fraction (arsenite + arsenate), and total arsenic for both cultivars (Fig. 1b). MMA and DMA were mostly undetected, and there was a very low recovery in rice grains during separation.<sup>6</sup> Therefore, to capture all unidentified arsenic compounds that were not separated, such as monothioarsenate (MTA), dimethylmonothioarsenate (DMTA), dimethyldithioarsenate (DDTA), or any other organic or inorganic arsenic compounds,<sup>54</sup> unidentified arsenic species were estimated by subtracting the inorganic arsenic fraction from the total arsenic.<sup>55,56</sup> In control systems (0.00% Fh), total arsenic in Norin rice grains was  $150.0 \pm 9.1 \mu\text{g As kg}^{-1}$ , whereas Sabharaj grains contained significantly ( $p < 0.01$ ) higher levels of total arsenic ( $239.9 \pm 16.0 \mu\text{g As kg}^{-1}$ ). The total arsenic uptake in rice grains from both cultivars in control soils was similar to what was observed in the field study conducted at the site where the soil was collected.<sup>32</sup> Inorganic arsenic content (arsenite + arsenate) was similar in both rice varieties (Norin:  $117.6 \pm 3.2 \mu\text{g kg}^{-1}$  and Sabharaj:  $116.6 \pm 2.9 \mu\text{g kg}^{-1}$ ) grown in the control soil. The Food and Drug Administration (FDA) guidance for inorganic arsenic levels in infant rice cereals is only below  $100 \mu\text{g kg}^{-1}$ ,<sup>57</sup> which was higher in both cultivars grown in control (no external Fh addition) soil.

In soils receiving Fh, rice grain showed significantly ( $p < 0.01$ ) lower inorganic arsenic concentrations in both the cultivars in 0.05% w/w Fh, Norin:  $13.8 \pm 1.1 \mu\text{g kg}^{-1}$  and Sabharaj:  $7.6 \pm 2.9 \mu\text{g kg}^{-1}$  and in 0.10% w/w Fh, Norin:  $16.4 \pm 2.2 \mu\text{g kg}^{-1}$  and Sabharaj:  $7.7 \pm 0.9 \mu\text{g kg}^{-1}$ . However, increased Fh was associated with a higher uptake of unidentified arsenic species in the rice grains of both cultivars than the control, which was significant ( $p < 0.01$ ) in Norin grains. Total arsenic in Norin grain was 32–37% lower in Fh-amended soil, while 35–58%

lower total arsenic was found in Sabharaj grains grown in Fh systems compared to those grown in control. Thus, significantly ( $p < 0.01$ ) lower total arsenic in rice grains for both cultivars was observed for both Fh amendments.

Lower inorganic arsenic, specifically arsenite, can benefit rice consumers as it is known to be the most carcinogenic among various arsenic species in rice grains.<sup>55</sup> Iron plaque can sequester inorganic arsenic, limiting its entry into the plant, while it has been reported to weakly adsorb organic arsenic species.<sup>58</sup> Increased uptake of organic arsenic species has been observed in a previous hydroponic study by Kerl *et al.*, 2019,<sup>10</sup> where a higher transfer rate from root to shoot of organic arsenic species, specifically DMA, MMA, and DMTA was observed in rice with iron plaque formation.<sup>10</sup> In that same study, MMA was mostly sequestered in the iron plaque in roots, with lower root-to-shoot transfer than no plaque roots. The study did not investigate the grain transfer of these organic arsenic species.<sup>10</sup> However, to the best of our knowledge, the increased uptake of unidentified arsenic species, which may include different forms of inorganic and organic arsenic species, in a soil-flooded system, has not been reported before. Individual organic arsenic species were not measured in the present investigation, though a similar mechanism observed in the Kerl *et al.*, 2019 study,<sup>10</sup> may predict the increase in unidentified arsenic species levels in Fh-amended soil.

### 3.2 Enrichment of iron layers on rice roots and implication on arsenic availability

In each sampling event, DCB extractions of roots and soils were carried out to measure reactive iron levels as compared to arsenic.<sup>29,59</sup> Extracts of roots and soil were measured for arsenic and iron (Fig. 2a–h). Extractable arsenic and iron concentrations in roots were significantly ( $p < 0.01$ ) higher under soils with elevated Fh than control for both cultivars. In Norin, extractable-arsenic and -iron in roots between two Fh-levels were only significantly ( $p < 0.01$ ) different on day 60 (root extractable-arsenic:  $7258 \pm 168 \mu\text{g kg}^{-1}$  (0.00%),  $12\,347 \pm 986 \mu\text{g kg}^{-1}$  (0.05%),  $14\,538 \pm 158 \mu\text{g kg}^{-1}$  (0.10%); root extractable-iron:  $24\,589 \pm 1586 \mu\text{g kg}^{-1}$  (0.00%),  $47\,258 \pm 478 \mu\text{g g}^{-1}$  (0.05%),  $53\,500 \pm 854 \mu\text{g g}^{-1}$  (0.10%)) and day 120 samples (root extractable-arsenic:  $20\,456 \pm 1008 \mu\text{g kg}^{-1}$  (0.00%),  $28\,256 \pm 508 \mu\text{g kg}^{-1}$  (0.05%),  $32\,500 \pm 1250 \mu\text{g kg}^{-1}$  (0.10%); root extractable-iron:  $52\,050 \pm 625 \mu\text{g kg}^{-1}$  (0.00%),  $62\,311 \pm 347 \mu\text{g g}^{-1}$  (0.05%),  $65\,206 \pm 545 \mu\text{g g}^{-1}$  (0.10%)). In Sabharaj roots, extractable-arsenic differed significantly ( $p < 0.01$ ) on all collected samples in 0.05% Fh ( $6857\text{--}26\,858 \mu\text{g kg}^{-1}$ ) and across all sampling events from 0.10% Fh ( $11\,582\text{--}29\,008 \mu\text{g kg}^{-1}$ ) soils. Sabharaj-root samples presented significantly ( $p < 0.01$ ) higher concentrations of extractable-iron for all sampling days 30, 60, and 90, and followed a similar trend to arsenic. These observations indicate a close link between iron plaque and Fh-availability in roots and extractable arsenic. Root-extractable iron levels between the rice varieties may also suggest variation in rhizosphere chemistry between the two cultivars, which has been noted to be different for *japonica* (Norin) and *indica*



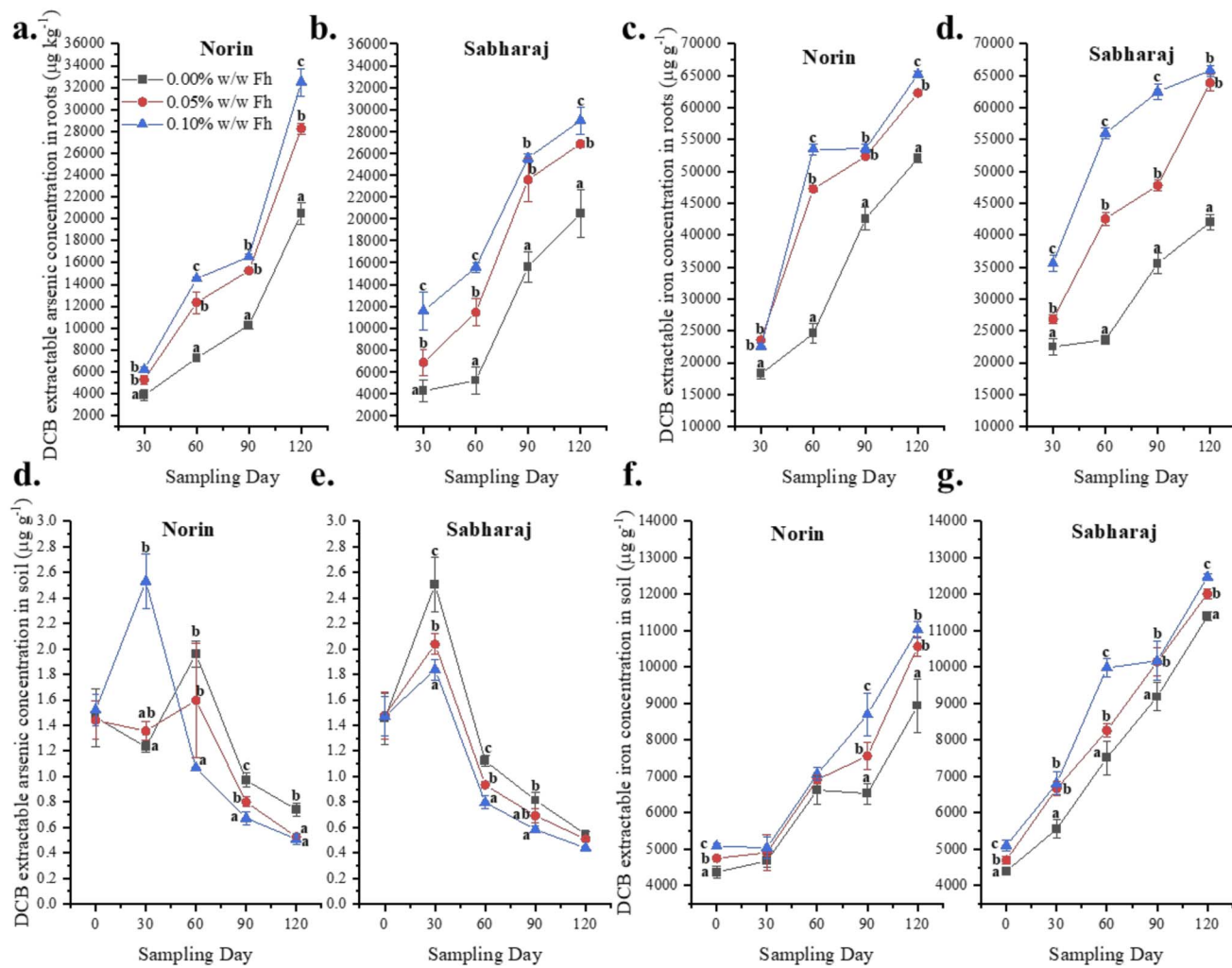


**Fig. 2** Rice roots were collected during destructive sampling, cleaned, dried, and dithionite-citrate-bicarbonate (DCB) extractable concentrations of arsenic were measured (a) Norin, (b) Sabharaj, and iron (c) Norin, (d) Sabharaj. Soil DCB extractions concentration of arsenic in (d) Norin, (e) Sabharaj, and iron in (f) Norin and (g) Sabharaj were measured to check iron plaque formation on rice roots. Fh elevated in soil presented significantly ( $p < 0.01$ ) higher concentration of extractable iron in root, promoting iron plaque formation. a, b, and c on top of data points show significantly different concentrations at  $p < 0.01$  as per the post hoc Tukey test.

(Sabharaj) rice varieties.<sup>23,60</sup> The higher extractable iron in roots correlated with the elevated levels of extractable iron in soils.

At day 0, the extractable-iron concentrations in soil were significantly different between three Fh-levels (0.00%:  $4366 \pm 172 \mu\text{g g}^{-1}$  (Norin),  $4400 \pm 100 \mu\text{g g}^{-1}$  (Sabharaj); 0.05%:  $4753 \pm 55 \mu\text{g g}^{-1}$  (Norin),  $4703 \pm 102 \mu\text{g g}^{-1}$  (Sabharaj), and 0.10%:  $5089 \pm 85 \mu\text{g g}^{-1}$  (Norin),  $5100 \pm 146 \mu\text{g g}^{-1}$  (Sabharaj)) under both cultivars. In soils, extractable-arsenic concentrations were similar on day 0 across three Fh-levels, and within levels previously observed in paddy soils.<sup>61</sup> However, soil extractable-arsenic concentration peaked significantly ( $p < 0.01$ ) on day 30 under Sabharaj across three Fh-levels, with the highest concentration in control ( $2.5 \pm 0.2 \mu\text{g g}^{-1}$ ), followed by 0.05% ( $2.03 \pm 0.08 \mu\text{g g}^{-1}$ ) and 0.10% ( $1.8 \pm 0.08 \mu\text{g g}^{-1}$ ) Fh system. As rice matured, the soil extractable arsenic concentration decreased, though a similar trend of soil extractable arsenic concentration continued to be observed across the systems.

Peak extractable arsenic was observed in 0.10% Fh under Norin on day 60 and followed the trend to Sabharaj as the experiment progressed. Low concentrations of DCB-extractable arsenic in soil compared to roots in the present study have been observed in previous studies.<sup>2,62,63</sup> An increase in DCB-extractable arsenic in soil under control can suggest a difference in rhizosphere chemistry due to thicker iron plaque in Fh systems, which can sequester available arsenic within the plaque.

### 3.3 Effect of adding ferrihydrite to soil on iron and arsenic species in irrigation water

Elevated Fh in the soil also impacted iron and arsenic species in the flooded irrigation water. Pore water samples from each tub were collected over time (30, 60, 90, and 120 days) under both cultivars Norin (Fig. 3a) and Sabharaj (Fig. 3b). For both rice varieties, total iron concentrations in water decreased over time across all Fh treatments. The high total iron in elevated Fh



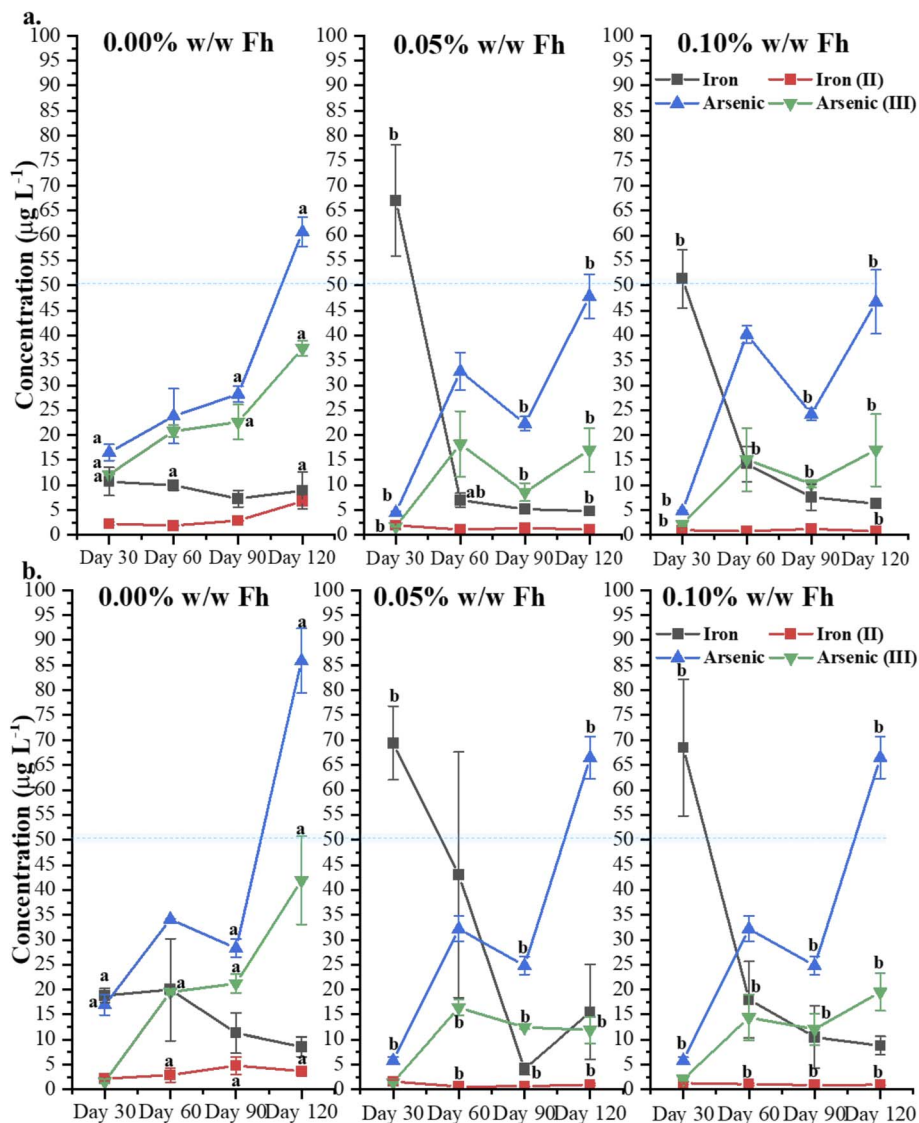


**Fig. 3** Concentration of total iron, arsenic, iron(II), and arsenite (As(III)) in irrigated pore water of (a) Norin and (b) Sabharaj. Irrigation water by design primarily contained arsenate (As(V)) (98.6% of total arsenic ( $50.2 \pm 2.1 \mu\text{g L}^{-1}$ ), shown as the blue line in the figure. Elevated Fh levels contained lower reduced arsenic in the water, which ensured lower uptake of arsenic in rice grains. a, b, and c on top of data points show significantly different concentrations at  $p < 0.01$  as per the post hoc Tukey test.

systems is likely from externally added Fh dispersed in the first irrigation water. On day 30, the elevated Fh systems showed significantly ( $p < 0.01$ ) higher total iron than the control. However, as the experiment progressed, total iron concentration in pore water across all three treatments under both rice varieties was similar. Iron(II) concentration remained low and relatively stable throughout the experiment for both varieties and all Fh treatments. Under both rice varieties, iron(II) concentration ranged from 33% to 89% of total iron in pore water of control on days 90 and 120. However, the high iron(II) trend was absent in elevated Fh systems.

Total arsenic concentration in applied irrigation water exhibited different trends depending on the Fh levels for the two rice varieties. In Norin, the total arsenic concentration in the control gradually increased as the experiment progressed,

peaking at day 120 ( $60.7 \pm 2.9 \mu\text{g L}^{-1}$ ). In contrast, in Sabharaj, the total arsenic in the control was dynamic, with a peak on days 60 ( $34.1 \pm 0.5 \mu\text{g L}^{-1}$ ) and 120 (highest value,  $85.9 \pm 6.4 \mu\text{g L}^{-1}$ ). Increased arsenic in pore water is likely from arsenic mobilized in the soil. The 0.05% and 0.10% Fh levels under both varieties presented a dynamic change in total arsenic over time, with an increase on days 60 and 120 and a decrease in concentration on other days. However, on day 30, the total arsenic concentration in Fh systems was significantly ( $p < 0.01$ ) lower than the control, indicating fresh reactive iron from added Fh sequestered arsenic well. A similar trend for arsenite concentration was observed in Fh systems, where it remained consistently low in both rice varieties, indicating that most arsenic present in the irrigation water was in arsenate form. In the control, specifically in Norin, arsenite was the major arsenic species in water,



**Fig. 4** Rice roots of Norin were collected on days 30, 60, 90, and 120 beneath control (0.00% w/w Fh), 0.05% w/w Fh, and 0.10% w/w Fh in soil. The red coloring of roots is visible early in the experiment in elevated Fh soils. Control soil roots become red at a later stage of the experiment. However, unlike elevated Fh systems, control roots were proportionately less red, indicating poor iron plaque in control roots.

ranging from 55% to 90%. In Sabharaj, arsenate was the primary species on day 30; however, arsenite became the major arsenic species in the water of the control as the experiment progressed, ranging from 57% to 73% of total arsenic.

Chemical equilibrium calculations using PHREEQC<sup>51</sup> provided an understanding of the various geochemical processes and predicted the equilibrium forms of iron and arsenic ions and minerals as irrigation water and soil interacted. The model-predicted arsenite concentrations aligned well with experimental findings (Table S3).<sup>53</sup> The model indicated an increasing saturation index of Fh in the water as the experiment progressed, suggesting that fresh reactive iron may form at the soil-root-water interface. This shift from negative to positive saturation index values is consistent with suspended Fh minerals throughout the growing period. The dynamic formation of fresh reactive iron can explain the significant impact on inorganic arsenic sequestration even with a low concentration of initial Fh, which seems to favor fresh reactive iron formation. The model suggests that fresh reactive iron may form as the

experiment progresses, which is well supported by the increased DCB-extractable iron concentration in the soil as the experiment progressed across three Fh levels (Fig. 2). A similar transformation of Fh has been observed in soil under unsaturated<sup>31</sup> and saturated<sup>64</sup> conditions. However, in this study, reduced iron concentration in water was lower compared to total iron, which is considered to be critical in driving Fh transformation reactions.<sup>65</sup> The results suggest that elevated Fh levels, especially at the higher 0.10% level, can effectively reduce arsenite concentrations in irrigation water under both rice varieties.

### 3.4 Probable mechanistic pathway of inorganic arsenic immobilization due to fresh reactive iron in soil

Changes in extractable iron levels in roots and soil, total iron, arsenite, and chemical equilibrium modeling suggests the enhanced iron plaque formation in both cultivars' roots under Fh systems. Clearly, systems with elevated reactive iron through



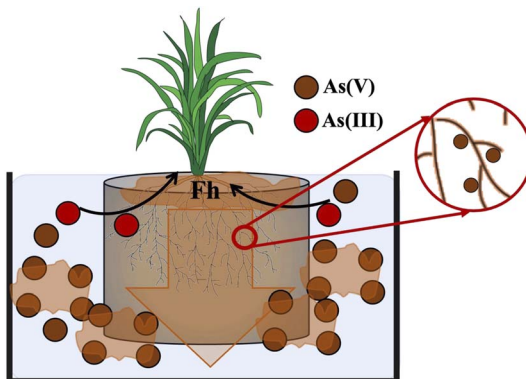


Fig. 5 Conceptual model presenting probable pathways of inorganic arsenic species immobilization due to elevated ferrihydrite (Fh) – a reactive iron nanomineral in paddy soils. The irrigation water primarily contained arsenate, a charged species at circumneutral pH. It forms an inner sphere complexation with freshly available Fh and is less available for transformation to arsenite. Additionally, slightly elevated Fh in paddy soil promotes the formation of iron plaque, which helps rice plants create a protective layer in immobilizing arsenic and reducing uptake, as observed in the DCB extraction of root samples. The elevated Fh also favors the formation of fresh Fh, as predicted by the geochemical equilibrium model and sustains the protective mechanism for reduced arsenic uptake.

added Fh showed iron plaque formation at an early stage compared to the control (Fig. 4 (shows Norin roots, and Fig. S2 shows Sabharaj roots)). Adding Fh, *i.e.*, 0.10% Fh, initiated root plaque formation faster than the lower level (*e.g.*, 0.05%) Fh, which can be seen in the collected root samples. The roots in the Fh-amended system initiated a high level of iron plaque formation within the first 30 days of the experiment, which was quantifiable from the iron concentration from DCB extraction of root samples, and is supported by the visible inspection of the roots. Low levels of Fh amendment, as observed in the present study, in unsaturated soil systems have been shown to reduce arsenic uptake by crops significantly.<sup>53</sup> A recent study has shown that pure Fh added to the soil, and when well mixed, can remain primarily in Fh form for a long time (the study measured it after 16 weeks).<sup>66</sup> A similar mechanism can be in play in the present study, and the low levels of Fh mixed with soil can last a long time to eliminate mobile arsenic forms effectively. Studies have also shown that fresh Fh in soil can lead to the formation of new reactive iron,<sup>31,53</sup> as observed in the present study, which can sustain the critical role of lowering inorganic arsenic uptake observed here.

The measured changes in composition of water and the chemical equilibrium model signify that authigenic Fh available in the soil of 0.05% and 0.10% Fh systems binds arsenate present in the irrigation water and mobilized arsenic coming from the paddy soil (Fig. 5). The strong complexation of arsenate on the Fh surface makes arsenic less available.<sup>67</sup> The Fh-bound arsenate most likely converted to organic arsenic species through methylation or thioarsenate formation (water contained sulfate (Table S1), sulfate:  $86 \pm 2 \text{ mg kg}^{-1}$ ) under continuously flooded conditions, as observed in other recent studies,<sup>68–75</sup> making them available for uptake in Fh systems.<sup>10</sup>

Organic arsenic compounds are readily translocated from rice roots to edible parts.<sup>76</sup> Therefore, if organic arsenic is available in Fh-systems, it can easily accumulate in the rice grains and most likely is part of the unidentified arsenic species. Decreased arsenite in the soil and water directly correlates to a decrease in the arsenic of mature rice grains of both cultivars in Fh systems. However, arsenite was observed in the control systems of both cultivars, making it available for uptake. As expected, compared to Sabharaj, Norin takes up less arsenic based on the variety. The soil to grain transfer factor of arsenic (Table S4) supports the proposed mechanism. Elevated Fh levels reduce arsenic translocation from shoots to final grain in both the cultivars, indicating reactive iron's critical role under different rhizosphere chemistry occurring in Norin and Sabharaj.<sup>23,60</sup>

The arsenic content and availability in soils for plants depend on various soil characteristics, including pH, redox potential, cation exchange capacity, and iron oxide concentration.<sup>77</sup> The soil pH was  $7.1 \pm 0.3$ , and Eh values at  $\sim 5 \text{ cm}$  depth were from  $-0.10 \text{ V}$  to  $0.28 \text{ V}$  in all three systems throughout the experiment timeline. When redox potential is high ( $>0.25 \text{ V}$ ), as observed in the flooded irrigation water in the present study, the predominant arsenic species is arsenate, which is less water-soluble and, thus, less bioavailable. However, solubility increases in alkaline pH or highly reducing conditions as arsenate is reduced to the more mobile arsenite. Under high redox potential, iron(II) oxidizes to iron(III), precipitating as iron oxides or hydroxides, forming an iron plaque on plant roots.<sup>21</sup> In this trial, the external supply of readily available Fh expedites the process of iron plaque formation. This iron plaque adsorbs inorganic arsenic, thereby reducing its uptake by plants, which is confirmed in the present study (Fig. 5). However, the specific trends and magnitudes of these reductions varied between the rice varieties, highlighting the importance of considering varietal differences in rhizosphere chemistry<sup>23,60</sup> when developing arsenic mitigation strategies in rice cultivation.

## 4. Conclusion

Our results highlight that small additions and minor variations in reactive iron levels in paddy soils can influence the type of arsenic accumulating in the final harvested rice grain. In the control paddy soil, total and inorganic arsenic transfer from soil to grain was significantly higher than in paddy soil with externally modified soil reactive iron with the addition of Fh. Lower levels of reactive iron in control lead to 42.6–51.2% higher arsenic in rice grains. Meanwhile, the addition of Fh provided additional adsorption and reactive sites for mobilized arsenic from the soil and irrigation water. The adsorption of arsenic onto reactive iron surfaces decreased concentrations of dissolved arsenic, leading to a decrease in arsenic uptake by rice. Identifying the Fh-bound inorganic arsenic transformation to organic arsenic species or any other unknown arsenic species in flooded paddy soil is beyond the scope of the present study and a critical future research question to understand the arsenic uptake mechanism. Besides, a slight increase in reactive iron levels was associated with unidentified arsenic species uptake, most likely Fh primed organic arsenic species formation.



Although multiple studies have confirmed that flooded irrigation results in the highest arsenic uptake by rice crops, flood irrigation is still the preferred mode of growing rice because of the ease of management in geographic areas where rice is grown.<sup>78</sup> Given the expected global growth in rice production, measures such as those observed in the present study under different rhizosphere chemistry are needed to ensure the safe quality of rice grains. Our work gave an insight into the details regarding arsenic transfer from soil to rice under slight differences in reactive iron levels under flooded conditions.

## Conflicts of interest

There are no conflicts to declare.

## Data availability

Data available on request from the authors.

Additional materials and methods are available in the SI. Table S1, water chemistry data of arsenate spiked tap water; Table S2, compares observed arsenic species in the reference material of the present study; Table S3, compares observed arsenite concentration to chemical model predicted values on day 30, 60, 90, and 120 in 0.00% w/w, 0.05% w/w and 0.10% w/w Fh systems; Table S4, soil to grain and shoot to grain transfer factor (TF) of arsenic in two rice varieties; Fig. S1, shows X-ray diffraction of synthesized Fh; Fig. S2, shows differences in iron plaque formation on roots of Sabharaj rice variety. See DOI: <https://doi.org/10.1039/d5em00475f>.

## Acknowledgements

This work was partially supported by the Nebraska Agricultural Experiment Station with funding from Hatch Multistate Research (Accession Number 1011588) through the USDA National Institute of Food and Agriculture. Malakar thanks the Nebraska Environmental Trust for partial salary support and the USDA NIFA AFRI-funded program (Accession number 1027886). Chemical analysis was conducted in the Water Sciences Laboratory, a core facility partially supported by the Nebraska Research Initiative.

## References

- 1 E. M. Muehe, T. Wang, C. F. Kerl, B. Planer-Friedrich and S. Fendorf, *Nat. Commun.*, 2019, **10**, 1–10.
- 2 X. Wang, T. Liu, F. Li, B. Li and C. Liu, *ACS Earth Sp. Chem.*, 2018, **2**, 103–111.
- 3 A. Malakar, B. Das, S. Islam, C. Meneghini, G. De Giudici, M. Merlini, Y. V. Kolen'ko, A. Iadecola, G. Aquilanti, S. Acharya and S. Ray, *Sci. Rep.*, 2016, **6**, 26031.
- 4 A. Spanu, L. Daga, A. M. Orlandoni and G. Sanna, *Environ. Sci. Technol.*, 2012, **46**, 8333–8340.
- 5 R. M. Couture, J. Rose, N. Kumar, K. Mitchell, D. Wallschläger and P. Van Cappellen, *Environ. Sci. Technol.*, 2013, **47**, 5652–5659.
- 6 P. N. Williams, A. H. Price, A. Raab, S. A. Hossain, J. Feldmann and A. A. Meharg, *Environ. Sci. Technol.*, 2005, **39**, 5531–5540.
- 7 Y.-G. Zhu, P. N. Williams and A. A. Meharg, *Environ. Pollut.*, 2008, **154**, 169–171.
- 8 F.-J. Zhao, S. P. McGrath and A. A. Meharg, *Annu. Rev. Plant Biol.*, 2010, **61**, 535–559.
- 9 D. R. Carrijo, N. Akbar, A. F. B. Reis, C. Li, A. C. M. Gaudin, S. J. Parikh, P. G. Green and B. A. Linquist, *F. Crop. Res.*, 2018, **222**, 101–110.
- 10 C. F. Kerl, T. B. Ballaran and B. Planer-Friedrich, *Environ. Sci. Technol.*, 2019, **53**, 13666–13674.
- 11 W. J. Liu, Y. G. Zhu, Y. Hu, P. N. Williams, A. G. Gault, A. A. Meharg, J. M. Charnock and F. A. Smith, *Environ. Sci. Technol.*, 2006, **40**, 5730–5736.
- 12 A. L. Seyfferth, S. M. Webb, J. C. Andrews and S. Fendorf, *Environ. Sci. Technol.*, 2010, **44**, 8108–8113.
- 13 R. D. Tripathi, P. Tripathi, S. Dwivedi, A. Kumar, A. Mishra, P. S. Chauhan, G. J. Norton and C. S. Nautiyal, *Metallomics*, 2014, **6**, 1789–1800.
- 14 M. Maisch, U. Lueder, A. Kappler and C. Schmidt, *Soil Syst.*, 2020, **4**, 28.
- 15 A. Mitra, S. Chatterjee, R. Moogouei and D. K. Gupta, *Agronomy*, 2017, **7**, 1–22.
- 16 M. Panthri and M. Gupta, *J. Environ. Manage.*, 2022, **316**, 115289.
- 17 D. Meng, F. Nabi, R. Kama, S. Li, W. Wang, Y. Guo, Z. Li and H. Li, *J. Hazard. Mater. Adv.*, 2024, **13**, 100398.
- 18 N. Yamaguchi, T. Ohkura, Y. Takahashi, Y. Maejima and T. Arao, *Environ. Sci. Technol.*, 2014, **48**, 1549–1556.
- 19 N. Yamaguchi, T. Nakamura, D. Dong, Y. Takahashi, S. Amachi and T. Makino, *Chemosphere*, 2011, **83**, 925–932.
- 20 L. Nie, S. Peng, M. Chen, F. Shah, J. Huang, K. Cui and J. Xiang, *Agron. Sustain. Dev.*, 2012, **32**, 411–418.
- 21 P. H. Masschelein, R. D. Delaune and W. H. Patrick, *Environ. Sci. Technol.*, 1991, **25**(8), 1414–1419.
- 22 A. R. Marin, P. H. Masschelein and W. H. Patrick, *Plant Soil*, 1993, **152**, 245–253.
- 23 J. Liu, X. Leng, M. Wang, Z. Zhu and Q. Dai, *Ecotoxicol. Environ. Saf.*, 2011, **74**, 1304–1309.
- 24 M. Hu, F. Li, C. Liu and W. Wu, *Sci. Rep.*, 2015, **5**, 1–10.
- 25 P. Kumarathilaka, S. Seneweera, A. Meharg and J. Bundschuh, *Water Res.*, 2018, **140**, 403–414.
- 26 P. Kumarathilaka, S. Seneweera, A. Meharg and J. Bundschuh, *Sci. Total Environ.*, 2018, **642**, 485–496.
- 27 F.-L. Meng, X. Zhang, Y. Hu and G.-P. Sheng, *Environ. Sci. Technol.*, 2024, **58**, 795–804.
- 28 M. S. Patzner, C. W. Mueller, M. Malusova, M. Baur, V. Nikeleit, T. Scholten, C. Hoeschen, J. M. Byrne, T. Borch, A. Kappler and C. Bryce, *Nat. Commun.*, 2020, **11**, 6329.
- 29 A. Malakar, D. D. Snow, D. Rudnick, B. Maharjan, M. Kaiser and C. Ray, *ACS Agric. Sci. Technol.*, 2024, **4**, 307–316.
- 30 S. Islam, S. Das, G. Mishra, B. Das, A. Malakar, I. Carluomagno, C. Meneghini, G. De Giudici, L. P. L. Gonçalves, J. P. S. Sousa, Y. V. Kolen'ko,



A. C. Kuncser and S. Ray, *Environ. Sci. Water Res. Technol.*, 2020, **6**, 2057–2064.

31 A. Malakar, M. Kaiser, D. D. Snow, H. Walia, B. Panda and C. Ray, *Environ. Sci. Technol.*, 2020, **54**, 13839–13848.

32 G. J. Norton, S. R. M. Pinson, J. Alexander, S. McKay, H. Hansen, G. Duan, M. Rafiqul Islam, S. Islam, J. L. Stroud, F. Zhao, S. P. McGrath, Y. Zhu, B. Lahner, E. Yakubova, M. Lou Guerinot, L. Tarpley, G. C. Eizenga, D. E. Salt, A. A. Meharg and A. H. Price, *New Phytol.*, 2012, **193**, 650–664.

33 T. Fukao, E. Yeung and J. Bailey-Serres, *Plant Cell*, 2011, **23**, 412–427.

34 A. Shrivastava, A. Barla, A. Majumdar, S. Singh and S. Bose, *Chemosphere*, 2020, **238**, 124988.

35 J. R. Rout and W. J. Lucas, *Planta*, 1996, **198**, 127–138.

36 P. Paul, B. K. Dhatt, M. Miller, J. J. Folsom, Z. Wang, I. Krassovskaya, K. Liu, J. Sandhu, H. Yu, C. Zhang, T. Obata, P. Staswick and H. Walia, *Plant Physiol.*, 2020, **182**, 933–948.

37 Z.-F. Yuan, W. Gustave, J. Boyle, R. Sekar, J. Bridge, Y. Ren, X. Tang, B. Guo and Z. Chen, *Chemosphere*, 2021, **269**, 128713.

38 M. S. Azam, M. Shafiquzzaman and H. Haider, *J. Environ. Manage.*, 2023, **343**, 118204.

39 W. Xiao, X. Ye, Z. Zhu, Q. Zhang, S. Zhao, D. Chen, N. Gao and J. Hu, *Sci. Total Environ.*, 2021, **788**, 147786.

40 G. Doran, P. Eberbach and S. Helliwell, *Chemosphere*, 2006, **63**, 1892–1902.

41 F. M. Michel, L. Ehm, S. M. Antao, P. L. Lee, P. J. Chupas, G. Liu, D. R. Strongin, M. A. A. Schoonen, B. L. Phillips and J. B. Parise, *Science*, 2007, **316**, 1726–1729.

42 H. Tamura, K. Goto, T. Yotsuyanagi and M. Nagayama, *Talanta*, 1974, **21**, 314–318.

43 D. Kutscher, S. McSheehy-ducos, J. Wills, D. Jensen and T. F. Scientific, 2012, 70001.

44 X. Yu, C. Liu, Y. Guo and T. Deng, *Molecules*, 2019, **24**, 926.

45 W. J. Liu, Y. G. Zhu, Y. Hu, P. N. Williams, A. G. Gault, A. A. Meharg, J. M. Charnock, F. A. Smith, Z. Chen, Y. G. Zhu, W. J. Liu and A. A. Meharg, *New Phytol.*, 2005, **165**, 91–97.

46 D. T. Heitkemper, N. P. Vela, K. R. Stewart and C. S. Westphal, *J. Anal. At. Spectrom.*, 2001, **16**, 299–306.

47 J.-H. Huang, G. Ilgen and P. Fecher, *J. Anal. At. Spectrom.*, 2010, **25**, 800.

48 K. M. Kubachka, N. V. Shockley, T. A. Hanley, S. D. Conklin and D. T. Heitkemper, *Elemental Analysis Manual: Section 4.11: Arsenic Speciation in Rice and Rice Products Using High Performance Liquid Chromatography-Inductively Coupled Plasma-Mass Spectrometric Determination. Version 1.1*. 2012, retrieved from <https://www.fda.gov/media/95197/download>.

49 S. Mukta and A. Gundlach-Graham, *J. Anal. At. Spectrom.*, 2024, **39**, 491–499.

50 A. J. Signes-Pastor, M. Carey and A. A. Meharg, *Food Chem.*, 2016, **191**, 128–134.

51 D. L. Parkhurst and C. A. J. Appelo, *Model. Tech. B.*, 2013, **6**, 497.

52 J. W. Ball and D. K. Nordstrom, *User's Manual for WATEQ4F, with Revised Thermodynamic Data Base and Text Cases for Calculating Speciation of Major, Trace, and Redox Elements in Natural Waters Open-File Report 91-183*, 1991.

53 A. Malakar, D. D. Snow, M. Kaiser, J. Shields, B. Maharjan, H. Walia, D. Rudnick and C. Ray, *Sci. Total Environ.*, 2022, **806**, 150967.

54 A. E. Colina Blanco, C. F. Kerl and B. Planer-Friedrich, *J. Agric. Food Chem.*, 2021, **69**, 2287–2294.

55 F. Cubadda, B. P. Jackson, K. L. Cottingham, Y. O. Van Horne and M. Kurzius-Spencer, *Sci. Total Environ.*, 2017, **579**, 1228–1239.

56 J. Wang, C. F. Kerl, P. Hu, M. Martin, T. Mu, L. Brüggenwirth, G. Wu, D. Said-Pullicino, M. Romani, L. Wu and B. Planer-Friedrich, *Nat. Geosci.*, 2020, **13**, 282–287.

57 FDA, *Arsenic in Food and Dietary Supplements*, FDA, <https://www.fda.gov/food/metals/arsenic-food-and-dietary-supplements>, accessed 8 July 2019.

58 F. A. Linam, M. A. Limmer and A. L. Seyfferth, *Plant Soil*, 2024, **502**, 397–415.

59 D. C. Amaral, G. Lopes, L. R. G. Guilherme and A. L. Seyfferth, *Environ. Sci. Technol.*, 2017, **51**, 38–45.

60 C.-H. Lee, Y.-C. Hsieh, T.-H. Lin and D.-Y. Lee, *Plant Soil*, 2013, **363**, 231–241.

61 J. Long, D. Zhou, Y. Huang, Z. Yi, D. Bin, Y. Luo, J. Wang, J. Deng and M. Lei, *Appl. Geochemistry*, 2022, **142**, 105311.

62 X. Tian, G. Chai, M. Lu, R. Xiao, Q. Xie and L. Luo, *Ecotoxicol. Environ. Saf.*, 2023, **254**, 114714.

63 X. Xu, C. Chen, P. Wang, R. Kretzschmar and F.-J. Zhao, *Environ. Pollut.*, 2017, **231**, 37–47.

64 A. R. C. Grigg, L. K. ThomasArrigo, K. Schulz, K. A. Rothwell, R. Kaegi and R. Kretzschmar, *Environ. Sci. Process. Impacts*, 2022, **24**, 1867–1882.

65 C. M. Hansel, S. G. Benner and S. Fendorf, *Environ. Sci. Technol.*, 2005, **39**, 7147–7153.

66 K. Schulz, W. Wisawapipat, K. Barmettler, A. R. C. Grigg, L. J. Kubeneck, L. Notini, L. K. ThomasArrigo and R. Kretzschmar, *Environ. Sci. Technol.*, 2024, **58**, 10601–10610.

67 A. Burnol, F. Garrido, P. Baranger, C. Joulian, M. C. Dictor, F. Bodéan, G. Morin and L. Charlet, *Geochem. Trans.*, 2007, **8**, 1–18.

68 N. Kumar, V. Noël, J. Besold, B. Planer-Friedrich, K. Boye, S. Fendorf and G. E. Brown, *ACS Earth Sp. Chem.*, 2022, **6**, 1666–1673.

69 J. M. León Ninin, A. Higa Mori, J. Pausch and B. Planer-Friedrich, *Sci. Total Environ.*, 2024, **943**, 173793.

70 X. Fang, A. E. Colina Blanco, I. Christl, M. Le Bars, D. Straub, S. Kleindienst, B. Planer-Friedrich, F.-J. Zhao, A. Kappler and R. Kretzschmar, *Environ. Pollut.*, 2024, **347**, 123786.

71 T. Arao, A. Kawasaki, K. Baba, S. Mori and S. Matsumoto, *Environ. Sci. Technol.*, 2009, **43**, 9361–9367.

72 X. Zhang, P. Zhang, X. Wei, H. Peng, L. Hu and X. Zhu, *Sci. Total Environ.*, 2024, **951**, 175500.

73 M. H. Hemmat-Jou, S. Liu, Y. Liang, G. Chen, L. Fang and F. Li, *Sci. Total Environ.*, 2024, **944**, 173873.



74 H. W. Langner and W. P. Inskeep, *Environ. Sci. Technol.*, 2000, **34**(15), 3131–3136.

75 K. Ito, M. Kuramata, H. Tanikawa, A. Suda, N. Yamaguchi and S. Ishikawa, *BMC Microbiol.*, 2024, **24**, 396.

76 T. Punshon, B. P. Jackson, A. A. Meharg, T. Warczack, K. Scheckel and M. Lou Guerinot, *Sci. Total Environ.*, 2017, **581–582**, 209–220.

77 A. Romero-Freire, M. Sierra-Aragón, I. Ortiz-Bernad and F. J. Martín-Peinado, *J. Soils Sediments*, 2014, **14**, 968–979.

78 G. Carracelas, J. Hornbuckle, M. Verger, R. Huertas, S. Riccetto, F. Campos, A. Roel and J. Agric, *Food Res.*, 2019, **1**, 100008.

